LA-5235-MS

INFORMAL REPORT

Continuous Crystallization of High Explosives

los alamos
scientific laboratory
of the University of California
LOS ALAMOS, NEW MEXICO 87544

UNITED STATES
ATOMIC ENERGY COMMISSION
CONTRACT W-7405-ENG. 36

In the interest of prompt distribution, this LAMS report was not edited by the Technical Information staff.

Printed in the United States of America. Available from
National Technical Information Service
U. S. Department of Commerce
5285 Port Royal Road
Springfield, Virginia 22151
Price: Printed Copy $3.00; Microfiche $0.95

LA-5235-MS
Informal Report
UC-26
ISSUED: April 1973

los alamos
scientific laboratory
of the University of California
LOS ALAMOS, NEW MEXICO 87544

Continuous Crystallization of High Explosives

by

L. E. Hatler

CONTINUOUS CRYSTALLIZATION OF HIGH EXPLOSIVES

by

L. E. Hatler

ABSTRACT

Nitroguanidine (NQ) is a high explosive that is commercially available in low bulk density form (0.20 to 0.30 g/cm^3). This low bulk density limits its usefulness as an explosive.

High bulk density NQ can be produced from a NQ-N, N-dimethylformamide-Versamid 125 system when crystallized in a mixed suspension mixed product removal crystallizer. Bulk densities ranged from 0.92 to 1.05 g/cm^3 for the operating conditions used.

The effect of agitator speed, growth rate, and solids concentration on nucleation rates was determined using a multiple linear regression technique. The resulting equation is: $B_o = 0.19\,(rpm)^{1.54}\,(G)^{1.68}\,(M_T)^{0.09}$. The result is consistent with postulated secondary nucleation mechanisms.

NOMENCLATURE

B_o	Nucleation rate, number per ml mother liquor per unit time
C	Concentration in exit mother liquor, g/ml solution
C_i	Concentration in feed solution, g/ml solution
C_s	Concentration from solubility diagram, g/ml solution in crystallizer
D	Constant relating to agitator speed
DMF	N, N-dimethylformamide
G	Growth rate, μ/min
i	Order of nucleation relating to growth rates
j	Order of nucleation relating to solids concentration
k_g	Constant
k_m	Constant
k_n	Constant
k_v	Constant relating to volumetric shape factor
L	Particle size, μ
M_T	Total weight of crystals per unit volume of mother liquor, g/ml
m	Mass of crystal, g
n	Population density, number per unit volume mother liquor per unit size
n(L)	Population density function
n_o	Nuclei density, number per unit size per ml mother liquor
Q_i	Flow rate into crystallizer, ml/min
Q(L)	Function relating product removal to size L

Q_o	Flow rate out of crystallizer, ml/min	V	Volume of crystallizer, liters
rpm	Agitator speed, revolutions per minute	W	Mass fraction
S	Supersaturation = $C-C_s$, g/ml of solution	x	Dummy variable
t	Time, min	ρ	Density, g/cm^3
		τ	Holding time, min

I. INTRODUCTION

A. Background

Nitroguanidine (NQ) is a high explosive that was first used by the Germans in World War I. Its main practical use is as an ingredient of flashless propellent mixtures.[1] It is also used as an explosive for various military applications.

The molecular weight of NQ is 104 and the empirical formula is $CH_4N_4O_2$. Jousselin[2] synthesized it first in 1877 by dissolving guanidine nitrate in fuming nitric acid through which nitrous oxide was bubbled. This solution was heated for a few minutes, after which it was poured into water to precipitate the product. The most practical current method of preparing NQ is that of adding guanidine nitrate to concentrated sulfuric acid.[3]

NQ has a crystal density of 1.77 g/cm^3.[4] In the production of NQ, which involves a final water crystallization, crystals are produced in a fine needle form having a bulk density of 0.20 to 0.30 g/cm^3.

A crystal product of this type has many characteristics that limit its usefulness. For instance, the detonation velocity of NQ at a density of 1.0 g/cm^3 is 5300 m/sec,[5] while the detonation velocity of trinitrotoluene (TNT) has a lower value of 5060 m/sec[6] at the same density. Ordinary TNT can be manually packed to this density, but the NQ, even when intensely pressed by mechanical methods, can be compressed to densities approaching 1.0 g/cm^3 only with difficulty. Further, its low weight per unit volume causes shipping and storage problems. Another disadvantage of this type of NQ is the interlocking of its fine needles, which makes it difficult to use in slurries for pouring into shells, bombs, or other containers.[7]

These problems can be alleviated if crystallization of NQ into a more useful form could be implemented. Pritchard and Wright[7] describe a procedure in which NQ is dissolved in boiling water and introduced into methanol. Bulk densities of 0.96 g/cm^3 have been produced by this method. Cave, Krotinger and McCaleb[8] reported the effects of varying the rate of crystallization of NQ from water to which wetting agents were added. However, the melting point of the product was lowered, indicating contamination.

The above studies were carried out in batch processes. It is often difficult to reproduce the product exactly, especially its crystal size distribution, habit, and purity, from batch to batch. A better method for studying crystal size distributions, habits, and purity would be found in a continuous process. A continuous mixed suspension mixed product removal (MSMPR) crystallizer is an ideal tool for studying crystallization processes.[9]

As in any process, material and energy balances are necessary to describe the system. In crystallization processes, however, material and energy balances do not provide an adequate description of the state of subdivision of the particulate matter. A balance involving crystals in discrete size ranges that can be related to operating conditions of the crystallizer is needed. This balance is called a numbers or population balance. The crystal size distribution, habit, and purity of NQ can be studied by incorporating the population

balance with the kinetics of formation and the growth rates of particles.

B. Population Balance

The development of the population balance can be facilitated by recognizing that as mass and energy must be conserved, so must the number of discrete particles.[10] A change of phase from liquid to solid in a solution crystallizer results in a collection of discrete particles of various sizes, shapes, and ages. By the proper representations of birth, growth, and death rates, one can account for all particles. Such an accounting is called a population balance.[11]

Since particle size is important in crystallization systems, the population of particles will be defined as a function of size. Let n(L) represent the number of particles as a function of size L per unit volume of solid-free liquid in a liquid-solid particulate system. This function is defined as the population density, and the number of particles found in size range L to L + dL in a volume of solid-free liquid V can be represented by

$$dN = Vn(L)dL \tag{1}$$

where N is the number of crystals, n(L) is the population density as a function of L (this function is yet to be determined), and V is the volume of liquid in the crystallizer.

The number of particles per unit volume of liquid in a finite range L_1 to L_2 can be found by dividing Eq. (1) by V and integrating

$$N(L_1, L_2) = \int_{L_1}^{L_2} n(L)dL \tag{2}$$

and, similarly, the total number of particles is

$$N_T = \int_0^{\infty} n(L)dL \quad . \tag{3}$$

If we assume that the mass, m, of each particle can be related to the cube of its size, then

$$m = \rho k_v L^3 \tag{4}$$

where ρ is the density of the particle and k_v is a shape factor.

The mass of particles in the size range L to L + dL in a volume of liquid V can be represented as

$$dm = \rho k_v L^3 n(L)dL \quad . \tag{5}$$

The mass in a finite range L_1 to L_2 can be found by integrating Eq. (5), thus

$$m(L_1, L_2) = \rho k_v \int_{L_1}^{L_2} L^3 n(L)dL \quad . \tag{6}$$

Similarly, the total mass can be found by

$$M_T = \rho k_v \int_0^{\infty} L^3 n(L)dL \quad . \tag{7}$$

The mass fraction, $W(L_1, L_2)$, and cumulative mass fraction, W(L), can be found from

$$W(L_1, L_2) = \frac{\rho k_v \int_{L_1}^{L_2} L^3 n(L)dL}{M_T} \tag{8}$$

and

$$W(L) = \frac{\rho k_v \int_0^{L} L^3 n(L)dL}{M_T} \quad . \tag{9}$$

A similar development can be made for the surface area of the particles and can be found in Ref. 10.

If an equation for n(L) can be determined, the development described above provides a convenient method for determining the number of particles from a screen analysis.

To develop an equation for n(L) using the population balance, a continuous MSMPR crystallizer is used.[9] Figure 1 schematically represents crystallizers of this type. They are characterized by a clear feed solution of constant composition, a well mixed slurry, and an unclassified product

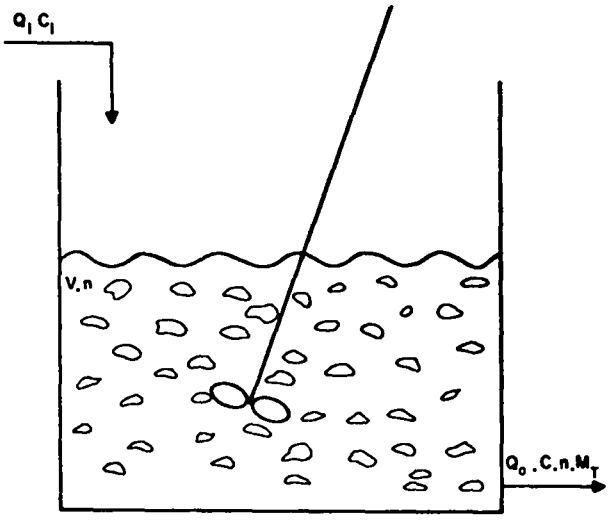

Fig. 1. Continuous mixed suspension mixed product removal crystallizer.

removal. The force driving the dissolved material to change to the solid phase can be provided by cooling the solution, evaporating the solvent, or adding a nonsolvent liquid to cause precipitation.

The classical statement of conservation,

$$\text{Accumulation} = \text{Input} - \text{Output} \qquad (10)$$

is now applied at steady state to the number of particles in an arbitrary size range, ΔL, and time interval, Δt: [12]

$$\underset{\text{INPUT}}{VG_1 n_1 \Delta t} = \underset{\text{OUTPUT}}{VG_2 n_2 \Delta t + Qn\Delta L\Delta t} \qquad (11)$$

where G is the linear growth rate and Q is the product flow rate. The number of crystals growing into a size range of interest is considered the input, while the output is represented by the number of crystals growing out of the range of interest plus the number of crystals removed from the crystallizer.

Dividing Eq. (11) by Δt and rearranging, we arrive at

$$\lim \Delta L \to 0 \; \frac{V(G_2 n_2 - G_1 n_1)}{\Delta L} + Qn = 0 \quad . \qquad (12)$$

Taking the limit as ΔL approaches 0

$$V\frac{d(Gn)}{dL} + Qn = 0 \quad . \qquad (13)$$

If we let $V/Q = \tau$, the holding time. Eq. (13) becomes

$$\frac{d(Gn)}{dL} + \frac{n}{\tau} = 0 \quad . \qquad (14)$$

McCabe[13] observed that crystals in suspension often grow at the same rate, regardless of their initial size, when subjected to the same conditions; that is, $G \neq G(L)$. This has become known as McCabe's ΔL law of crystal growth. Assuming that it holds in this study, Eq. (14) reduces to

$$\frac{dn}{dL} + \frac{n}{G\tau} = 0 \quad . \qquad (15)$$

Defining n_o to be the population density of embryo-size crystals and letting the size of these crystals approach zero, Eq. (15) can be integrated

$$\int_{n_o}^{n} \frac{dn}{n} = -\int_{0}^{L} \frac{dL}{G\tau} \quad . \qquad (16)$$

Upon integration we arrive at

$$n = n_o \exp\left(-\frac{L}{G\tau}\right) \quad . \qquad (17)$$

This form of the equation has been used successfully by many investigators.[9, 11, 14, 15, 16, 17]

From a screen analysis of product crystals, population densities at mean sizes of screen fractions can be calculated by using an equation developed from Eq. (8)

$$n = \frac{WM_T}{\rho k_v \bar{L}^3 \Delta L} \qquad (18)$$

where ΔL is the difference between the screen under consideration and the size of the screen immediately above, and $\bar{L}$ is the average of these two sizes.

Population densities obtained from Eq. (18) are plotted as a function of size $\bar{L}$ on a semilog plot. The resulting straight line has a slope of $-1/G\tau$ and an intercept of n_o.

Data often deviate from this relationship; however, an alternative method, proposed by Randolph and Larson,[10] can be developed as follows:

If we substitute Eq. (17) into Eq. (7), we get

$$M_T = \rho k_v n_o \int_0^\infty L^3 \exp\left(-\frac{L}{G\tau}\right) dL \quad . \tag{19}$$

Letting $x = (L/G\tau)$, Eq. (19) becomes

$$M_T = k_v n_o (G\tau)^4 \int_0^\infty X^3 e^{-x} dx \quad . \tag{20}$$

Recognizing the integral as the gamma function, we can evaluate it as 3 factorial. Eq. (20) will reduce to

$$M_T = 6\rho k_v n_o (G\tau)^4 \quad . \tag{21}$$

By using a cumulative size distribution plot, weight percent for a given size can be determined. Using a gamma function table and the weight percent, w(x), chosen from the distribution plot, a corresponding x can be found. From $x = (L/G\tau)$, a value for G can be calculated for a given holding time in the crystallizer. M_T is independently measured from experimental conditions in the crystallizer. By using Eq. (21), a value for n_o can be calculated. A value for the nucleation rate, B_o, can be obtained from the nuclei density, n_o, as follows:

$$\frac{dn}{dt} = \frac{dn}{dL} \cdot \frac{dL}{dt} = n_o G \quad . \tag{22}$$

Evaluating Eq. (22) at zero size gives the nucleation result as

$$B_o = n_o G \quad . \tag{23}$$

This equation assumes that all the crystals enter the distribution as nuclei and grow to the larger particles.

C. Nucleation Kinetics

Nucleation or crystal formation can take place by homogeneous, heterogeneous, or secondary mechanisms. Homogeneous nucleation occurs spontaneously from highly supersaturated solutions. When it occurs, all the dissolved solids drop from solution. Homogeneous nucleation does not seem to occur in industrial crystallizers, which generally operate at lower values of supersaturation. Heterogeneous nucleation is nucleation that is catalyzed by foreign materials such as dust particles. Both homogeneous and heterogeneous nucleation occur at supersaturation levels that are too high for good crystal growth. Secondary nucleation occurs when nucleation is induced by the presence of crystalline solid or seed crystals. In most industrial crystallization processes, secondary nucleation is the dominant mechanism of crystal generation.[17]

Mason and Strickland-Constable[18] have suggested three types of secondary nucleation. The first is initial breeding, caused by washing crystal dust from dry seed crystals placed in solution. The second type is the result of breakage of needle and dendritic growths from crystal surfaces. The third is collision breeding, induced by collisions of crystals with each other and with solid portions of the crystallizer.

In secondary nucleation, collision breeding can be caused by crystal collisions with impeller blades or other surfaces on the crystallizer, as well as by crystal-crystal contacts. Clontz and McCabe[19] showed that a large number of nuclei were produced from crystal-crystal contact.

The NQ forms small twinned needle crystals when produced by the rapid addition of water to saturated NQ solutions. Fine dendrites are produced by this method, which is characteristic of high supersaturation levels. These supersaturation levels generate nuclei by a homogeneous nucleation mechanism.

The longer retention times and better mixing, which can be achieved in a cooling crystallization process for NQ, favors the production of larger crystals.

For mixed suspension systems, growth rates are very nearly linear functions of supersaturations:

$$G = k_g S \quad . \tag{24}$$

It has also been shown that the dependence of secondary nucleation on supersaturation in mixed magma crystallizers can be expressed by simple power law kinetic models:[11]

$$B_o \equiv \frac{dN}{dt} = k_m S^i \quad . \tag{25}$$

Nucleation and growth are occurring in the same environment; therefore, they are dependent on the same level of supersaturation and Eqs. (24) and (25) can be combined to give

$$B_o = k_n G^i \tag{26}$$

or

$$n_o \equiv \frac{B_o}{G} = k_n G^{i-1} \quad . \tag{27}$$

The MSMPR crystallizer does not distinguish between nucleation mechanisms. Further, experiments such as Clontz's[19] and Mason's[18] do not provide empirical kinetic correlations for nucleation rates that can be used in determining operating conditions and scale-up for industrial crystallizers. However, Youngquist and Randolph[17] have tried to bridge this gap between the mechanism studies and purely empirical kinetics by measuring the output suspension from a MSMPR crystallizer in situ with a Coulter counter which is capable of size measurement down to 3 μ. These studies produced the relationship for an ammonium sulfate-water system:

$$B_o = k_v (\text{rpm})^{7.84} G^{1.22} M_T^{0.98} \quad . \tag{28}$$

The strong dependence of nucleation rate on the stirrer speed provides substantial evidence that secondary nuclei are generated by collisions of seed crystals with the impeller blades.

Rates of nucleation and growth can also be varied by using surface and ionic additives. However, we do not yet know how to select an additive that will produce a given effect in a given system. Shor and Larson[16] found that ionic additives increase the crystal size (reduce nucleation) and surface active agents decrease the crystal size (increase nucleation) on potassium sulfate. Liu and Botsaris[15] used a MSMPR crystallizer to determine the effects of lead ion (Pb++) additives on the nucleation and growth rates of NaCl. They found that the nucleation and growth rates, as well as the dominant sizes, can be correlated by a simple power function of impurity concentration. The exponent in their nucleation rate equation [same as Eq. (27)] was a constant independent of impurity concentration. The relative orders of nucleation and growth rates were the only things that changed.

II. PRESENT STUDY

A MSMPR crystallizer was designed and built for use with high explosives. The functionality of the equipment was tested with an ammonium sulfate-water-methanol system before using an explosive material. This was done to ensure that explosives could be handled safely in the system.

Using the population balance method described here, nucleation and growth rates were determined, and the nucleation kinetic property, i, from Eq. (27) was found to be 4.8. This compares well with a value of 4.0 reported by Larson, Timm, and Wolff.[14] It also compares well with a value reported by Robinson and Roberts as between 4 and 5.[20] From these experiments we concluded that the equipment described here is an efficient MSMPR crystallizer.

On the basis of an unpublished report describing work performed in a batchwise manner, N,N-dimethylformamide (DMF) was the solvent chosen for the crystallization of NQ for this study. The solubility of NQ in DMF is an order of magnitude higher than its solubility in water. Figure 2 shows the solubilities as a function of temperature for NQ in DMF and water. Crystallizing NQ from water (by the batch method) also caused problems in the thermal stability of the product. The DMF-NQ crystallization process done batchwise gave much better thermal stability than the water process.

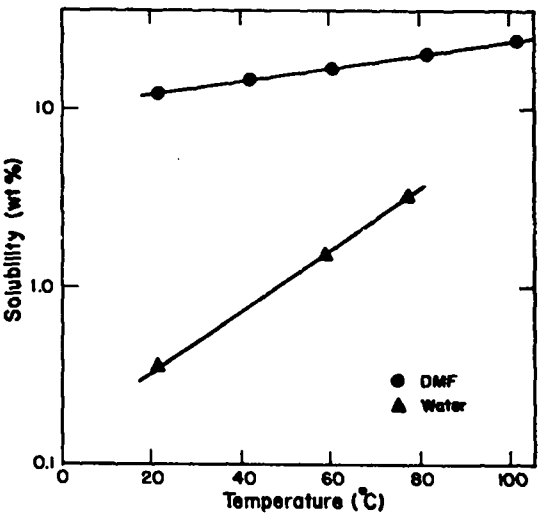

Fig. 2. Solubility of NQ in DMF and water.

The objectives of this study are to produce a high bulk density crystal and to determine the nucleation kinetics for the NQ-DMF system.

Preliminary runs indicated that a concentration of 20 wt% NQ in DMF would be the optimum operational feed concentration. Holding time and agitator speed were picked as variables in the study of the nucleation kinetics. The aim was to determine whether the agitator speed produced an observable effect on the nucleation kinetics when screen analysis was the method of particle size characterization.

The first series of runs using NQ-DMF produced crystals of low bulk densities. These crystals were twinned and agglomerated. This will be discussed in the Results section.

Versamid 125 was then added in an attempt to modify the crystal habit. Versamid is a polyamide resin that is used as a wetting agent and as a curing agent for epoxies. It is a condensation polymer of dimerized linoleic acid and ethylene diamine.[21] Blocky single crystals with high bulk densities were produced by this method. Photomicrographs and values for bulk densities will be reported in the Results section,

Six runs were performed with constant NQ-DMF-Versamid concentrations in the feed solution. Versamid concentration in the feed solution was 0.01 wt% and the NQ was nominally 20 wt%. Agitator speeds of 200, 250, and 300 rpm were selected. Holding times of 18 and 30 min at each speed were used.

III. EXPERIMENTAL EQUIPMENT AND PROCEDURE

A. Apparatus

Figure 3 shows a process flow diagram of the continuous MSMPR crystallizer used for these studies. Feed tanks A and B are 190-liter stainless steel vessels. The tanks are jacketed for solution heating or cooling. Operating temperature ranges from 20 to 100°C. The receiver tank is identical to the feed tanks except that its capacity is 380 liters. Figure 4 is a photograph of the apparatus.

The crystallizer reactor is a jacketed cylindrical stainless steel vessel 35.6 cm high by 25.4 cm diam. Three baffles are equally spaced 120° around the periphery of the crystallizer. An 18-cm-high by 16-cm-wide cooling coil is placed inside the crystallizer. The agitator, placed inside the coil, circulates the solution up the annulus and down the inside of the coil. A Dynalco tachometer indicates the agitator rpm.

The volume of the liquid in the crystallizer varies between 7.8 and 8.0 liters, because a liquid level control device periodically operates the discharge valve. Crystallizer temperature is controlled by the flow of hot and cold water mixed through two control valves. Temperature is held at ±2°C. Cooling water is circulated through the jacket and the coil inside the crystallizer.

The pumps in the system are Hills-McCanna double-headed diaphragm pumps with a single motor. Each head has an independent stroke adjustment, thus giving an equivalent of four pumps with two motors. Capacity of the recirculation pump (P-1) is 22 liters per minute. This pump transfers solution through an in line Pall filter to

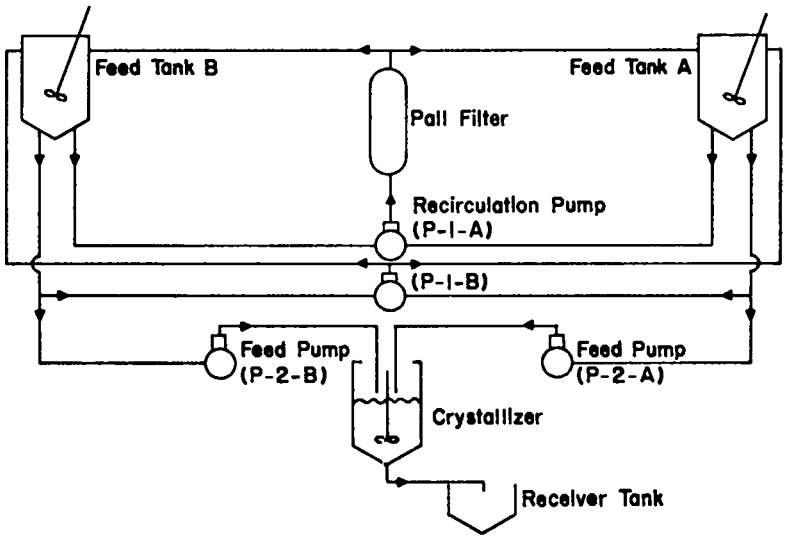

Fig 3. Process flow diagram of the crystallizer.

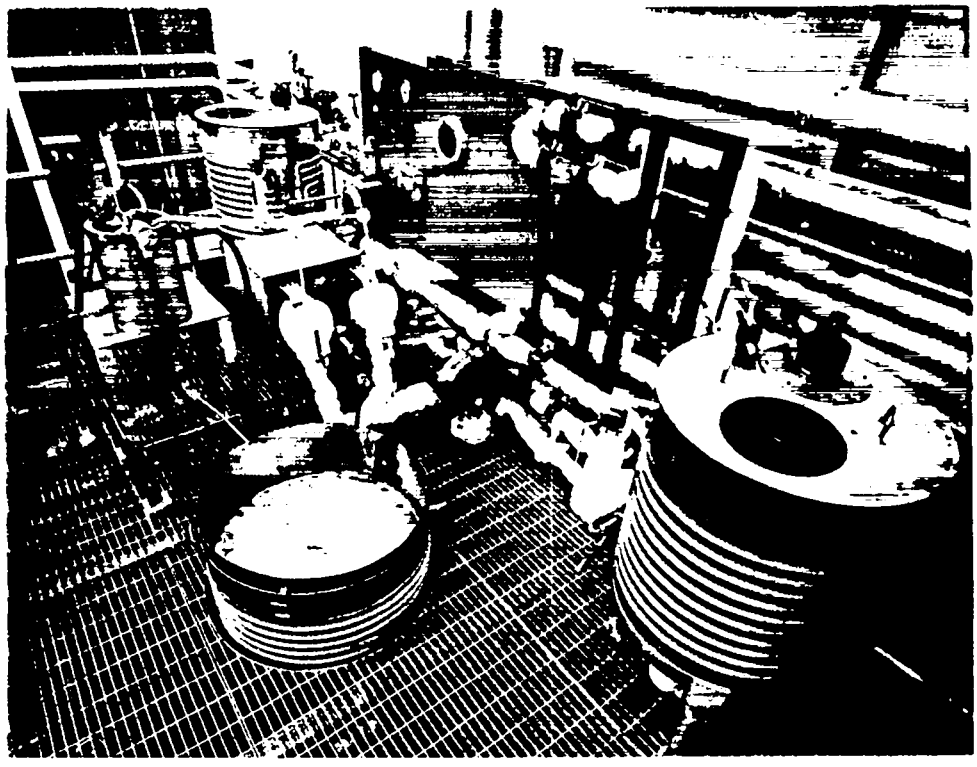

Fig. 4. Crystallizer system.

remove solid impurities. The crystallizer feed pump (P-2) has a capacity of 500 ml/min.

In this system crystallization can be accomplished either by cooling the hot saturated solution or by adding another nonsolvent liquid, causing precipitation of the desired product.

B. Material

The NQ packaged in 22.7-kg drums was purchased from Cyanamid of Canada Limited.

Technical grade DMF was purchased from Matheson, Coleman, and Bell.

Versamid 125 was purchased from General Mills, Inc., Chemical Division.

C. Procedure

Ninety-one kilograms of DMF was placed in feed tank A and heated to 90°C. The circulation and feed pumps were turned on and the discharge from both pumps was directed back into the feed tank. This allowed the feed and circulation lines to be heated to operating temperatures before the introduction of the NQ.

Twelve grams of Versamid 125 was then added to the hot DMF and the solution was allowed to circulate for 30 min. NQ in the amount of 22.7 kg was added to the DMF-Versamid solution. The entire solution was allowed to circulate for another 30 min to ensure homogeneity. The feed pump was adjusted to the flow rate to give the desired holding time. The agitator was set to the desired speed as indicated by the tachometer. The crystallizer was charged with seed crystals and mother liquor, corresponding to the slurry concentration expected during the run.

The feed was then directed to the crystallizer and allowed to run for 10 holding times. Samples were taken from the discharge of the crystallizer by use of a stainless steel Buchner-type funnel. The funnel has a 400-mesh stainless steel screen for filtration. After the mother liquor was drawn off, the crystals were washed in butyl acetate and placed in a vacuum oven to dry.

The sample was wet screened using butyl acetate as the transfer fluid. The flow rate was approximately 150 ml/min of butyl acetate. Each screen was washed for 2 min and then removed from the stack. The openings in the screens were 710, 500, 350, 250, 177, 125, 88, 62, 44, and 30μ.

The feed concentration of NQ was nominally 20 wt%. Versamid 125 concentration was 0.01 wt%. A sample of feed solution was evaporated to dryness and the residual NQ weighed to determine the actual feed concentration.

Agitator speeds of 200, 250, and 300 rpm were maintained at each of two holding times for the determination of nucleation kinetics. The holding times were nominally 18 and 30 min.

IV. RESULTS

A. Bulk Density

Six preliminary runs were conducted using NQ dissolved in DMF. Table 1 shows the bulk densities of the crystals produced under various operating conditions.

The product crystals exhibited twinned and multicrystal habits. The larger crystals were agglomerated into snowball-like masses, and smaller crystals were a fine, twinned, needle-like product. The combination of snowball and slender needle forms gave low bulk densities. Figure 5 is a photomicrograph of the crystals.

TABLE I

BULK DENSITIES AND OPERATING CONDITIONS FOR NQ-DMF SYSTEM

Run	Holding Time (min)	Temperature (°C)	rpm	Feed Concentration (wt%)	Bulk Density (g/cm^3)
1	15	25	200	19	0.54
2	20	25	300	18	0.25
3	20	15	250	19	0.23
4	40	15	250	20	0.13
5	20	15	200	17	0.30
6	40	30	200	17	0.35

Fig. 5. Crystals produced from NQ-DMF system.

The product offered no advantage over the commerical NQ and therefore was not acceptable.

In an attempt to transform the NQ from a multicrystal to a single-crystal habit, Versamid 125 was added. We hoped that the Versamid, which is used as a wetting agent in some applications, would wet the surface of the nuclei and inhibit further nucleation on the surface without affecting the growth rate.

Six runs were made using the NQ-DMF-Versamid system. The feed concentration was established as 20 wt% NQ in DMF. The concentration of Versamid was 0.01 wt%. The concentration of the feed was measured by evaporating a known weight of feed solution to dryness and weighing the residue. Table II gives the bulk densities of the product crystals and the operating conditions used to produce these densities.

The products were blocky, single crystals of high bulk densities. Figure 6 shows a crystal

TABLE II

BULK DENSITIES AND OPERATING CONDITIONS FOR NQ-DMF-VERSAMID SYSTEM

Run	Holding Time (min)	rpm	Feed Concentration (wt%)	Bulk Density (g/cm^3)
7	18	200	19.98	1.02
8	19	250	19.20	1.04
9	18	300	19.60	1.04
10	30	200	19.37	1.01
11	30	250	19.80	0.963
12	30	300	18.71	0.92

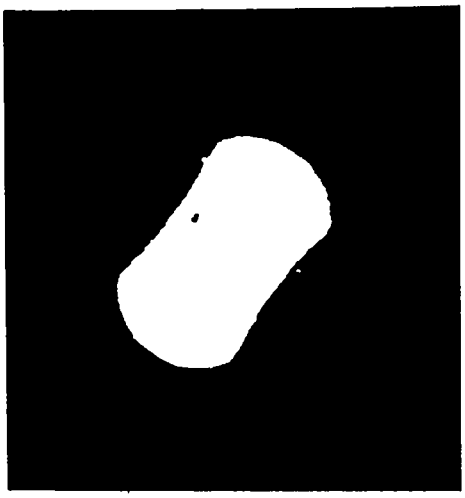

Fig. 6. Crystals produced from NQ-DMF-Versamid system.

produced by this system. A few of the larger crystals in these runs were slightly twinned, but not to the extent that occurred with the NQ-DMF system.

B. Nucleation Kinetics

Because of the multicrystal growth, we felt that the NQ-DMF system did not produce crystals that would give meaningful nucleation kinetics. Population density plots, made for a few runs, showed a distribution skewed toward larger sizes due to multicrystal growth.

Nucleation kinetics were determined for the NQ-DMF-Versamid system only. Size distribution data from screen analysis were used to determine population densities. The appendix contains data

obtained from screen analysis for the six runs plotted as cumulative weight percent. Population densities for the various size fractions up to size 214 μ were calculated from Eq. (18). Crystals larger than 214 μ exhibited slight twinning and were not used in the calculations. More than 99% of the crystal population occurs in the screen fractions up to 214 μ.

Figures 7 through 12 show the population densities versus crystal size for these runs.

The data were fitted with a least squares computer program and plotted on semilog paper. The growth rates were calculated from the known holding times and the slope, which was equal to $1/G\tau$. The nuclei density was the intercept on these plots.

To test the mass balance for these runs, the total solids concentration, M_T, was calculated from Eq. (21). Nuclei density and growth rates obtained from population density plots were used for the calculations. Since crystals larger than 214 μ were not considered, the calculated value of M_T was, in all cases, slightly lower than the experimentally measured value.

Table III contains the operating conditions and nucleation kinetics for the NQ-DMF-Versamid system.

Using Eq. (23), values for nucleation rates were calculated. Because of secondary nucleation considerations, the effect of the agitator speed on the nucleation rates was investigated. Figure 13 is a plot of the nucleation rate versus agitator speed. The two distinct curves represent high growth rates with short holding times (high driving forces) and low growth rates with long holding times (low driving forces).

An increase in nucleation rates was observed as agitator speeds were increased at high driving forces. At conditions of lower driving forces, the agitator speed seemed to have no effect on nucleation rates.

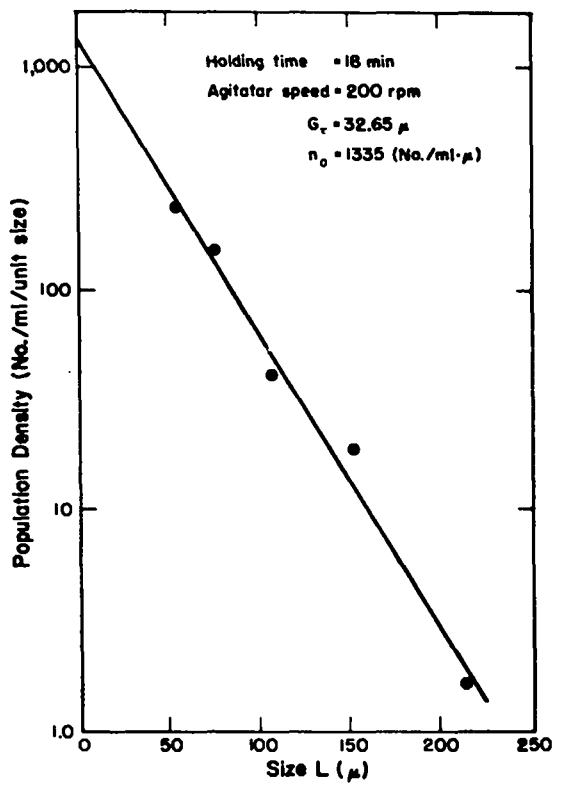

Fig. 7. Population density for run 7.

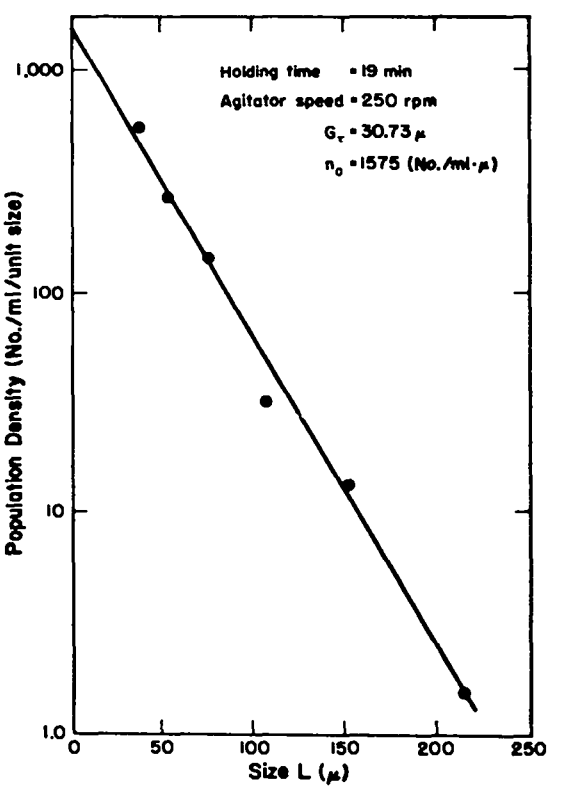

Fig. 8. Population density for run 8.

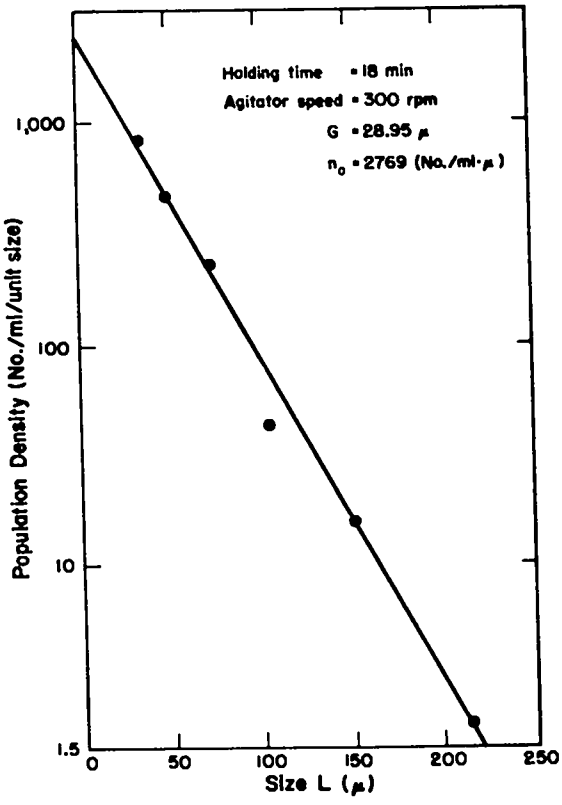

Fig. 9. Population density for run 9.

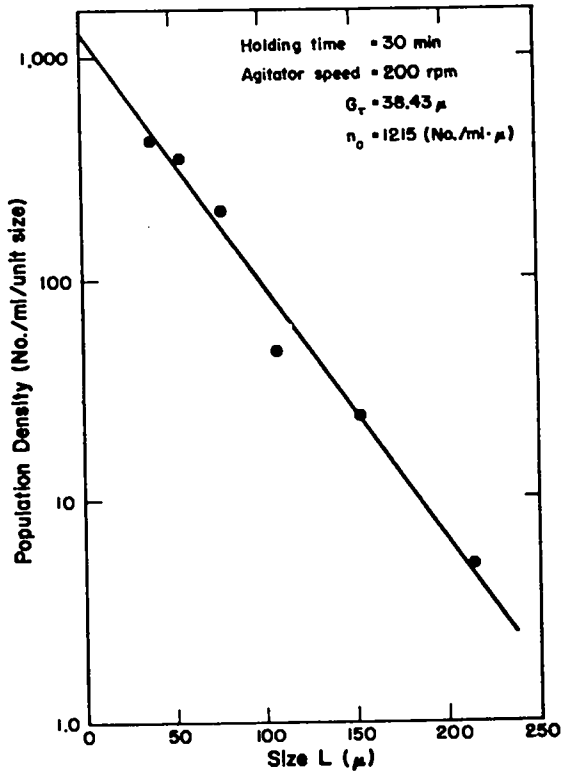

Fig. 10. Population density for run 10.

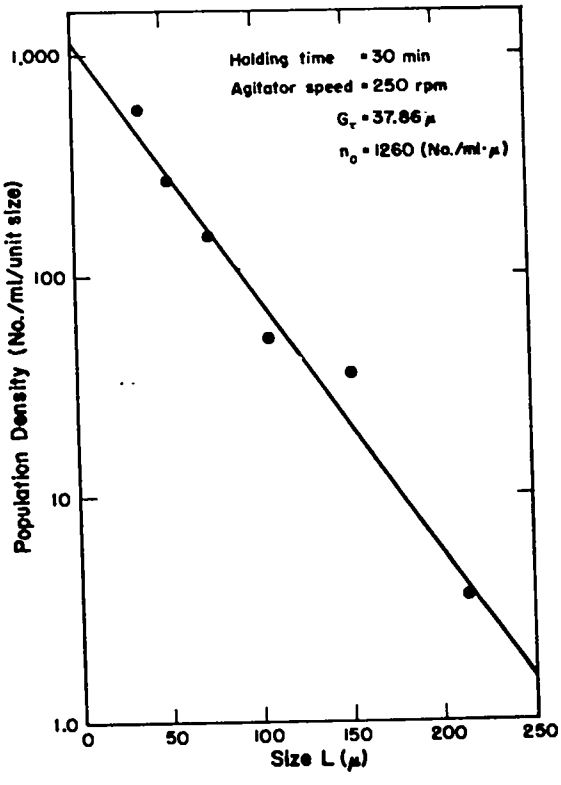

Fig. 11. Population density for run 11.

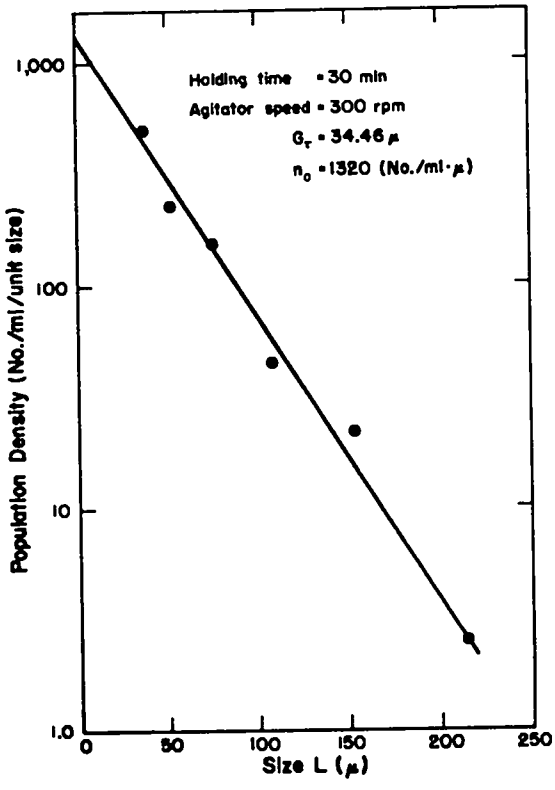

Fig. 12. Population density for run 12.

TABLE III

NUCLEATION KINETICS FOR NQ-DMF-VERSAMID SYSTEM

Run	Holding Time (min)	Agitator Speed (rpm)	G (μ/min)	n_o (No./ml·μ)	M_T Experimental (g/ml)	M_T Calculated (g/ml)
7	18	200	1.81	1335	0.0230	0.0161
8	19	250	1.62	1575	0.0168	0.0149
9	18	300	1.61	2769	0.0231	0.0206
10	30	200	1.28	1215	0.0325	0.0281
11	30	250	1.26	1260	0.0336	0.0260
12	30	300	1.15	1320	0.0225	0.0198

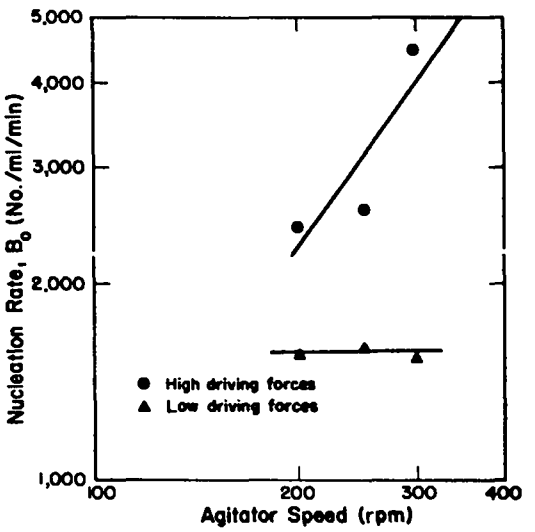

Fig. 13. Effect of agitator speed on nucleation rate.

A multiple linear regression analysis was applied to the data, and the result, described in a form similar to Eq. (28), is shown as

$$B_o = (0.19)\,(\text{rpm})^{1.54}\,(G)^{1.68}\,(M_T)^{0.09} \quad . \quad (29)$$

These results, plotted as $B_o/(\text{rpm})^{1.54}(M_T)^{0.09}$ versus G, appear in Fig. 14.

C. Yield

The yield from a MSMPR crystallizer can be obtained from a material balance. The weight of NQ in the inlet stream must equal the weight of NQ

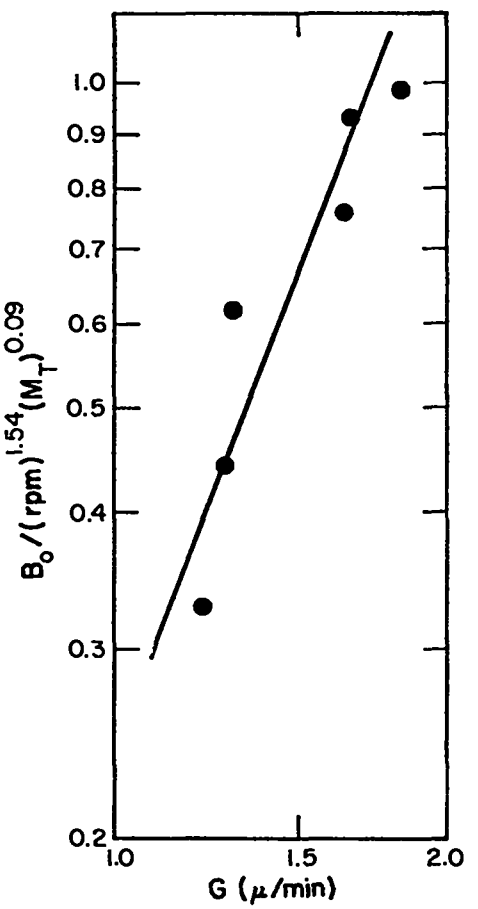

Fig. 14. Nucleation rate versus growth rate.

in the outlet stream plus the weight of solids removed as product.

The concentration of NQ in the mother liquor can be found from

$$Q_o C = Q_i C_i - Q_o M_T \qquad (30)$$

where C is the concentration of the NQ dissolved in the mother liquor, C_i is the NQ concentration in the feed stream, and M_T is the concentration of solids leaving the crystallizer. Q_i and Q_o are the flow rates into and out of the crystallizer, respectively.

The yield is equal to the NQ produced, divided by the total amount of NQ available for crystallization. Thus,

$$\text{yield} = \frac{Q_i C_i - Q_o C}{Q_i C_i - Q_o C_s} \qquad (31)$$

where C_s is the concentration at the saturation temperature. At steady state, the flow rate in, Q_i, equals the flow rate out, Q_o, and Eq. (31) reduces to

$$\text{yield} = \frac{C_i - C}{C_i - C_s} \quad . \qquad (32)$$

Table IV gives the values for the yield for the six runs. The low values are typical of Class I crystallizers, in which a measurable stable supersaturation exists. In Class II crystallizers with immeasurable supersaturations, the value of C approaches C_s and high yields result.

TABLE IV

PRODUCT YIELDS FOR NQ-DMF-VERSAMID SYSTEM

Run	Holding Time (min)	Yield (%)
7	18	33
8	19	27
9	18	34
10	30	49
11	30	47
12	30	40

A sample of mother liquor was evaporated to dryness and the residual NQ weighed. The weight fraction of NQ in the mother liquor was 0.167. The weight fraction of NQ in the feed was 0.198. From M_T, as calculated by Eq. (30), and a measured density of 0.985 g/cm^3 for the mother liquor, the weight fraction of solids leaving the crystallizer was calculated to be 0.031. The same weight fraction was experimentally measured as 0.032.

Growth rates for these runs were plotted as a function of supersaturation in Fig. 15. Data from this plot, coupled with the population balance and the mass balance, can be used to simulate NQ crystallization in crystallizers of arbitrary configurations. Thus, using the crystal-size distribution algorithm developed by Randolph and Larson,[10] the following set of equations would be sufficient to describe the size distribution, production, and yield in a Class I steady-state backed mixed crystallizer:

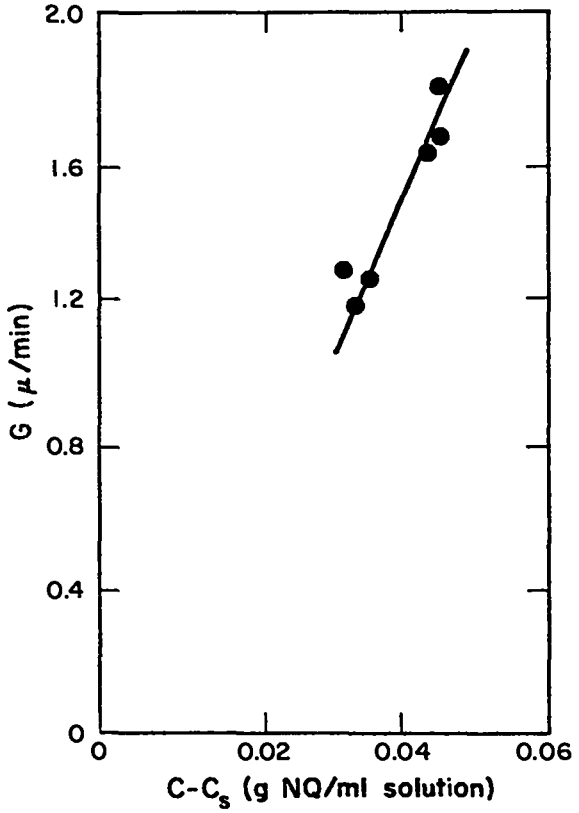

Fig. 15. Growth rate versus supersaturation ($C-C_s$).

Population Balance	$V \frac{d(Gn)}{dL} = Q_i N_i - \left[Q_o(L)\right] n$	(33)
Mass Balance	$Q_i C_i = Q_o C + \rho k_v \int_0^\infty \left[Q_o(L)\right] nL^3 dL$	(34)
Nucleation Kinetics	$B_o = k_n (rpm)^D G^i M_T^j$	(35)
Growth Kinetics	$G = k_g (C - C_s)$	(36)
Solids Concentration	$M_T = \rho k_v \int_0^\infty nL^3 dL$	(37)
Production	$P = \rho k_v \int_0^\infty Q_o(L) nL^3 dL$	(38)
Yield	$Yield = \frac{C_i - C}{C_i - C_s}$	(39)

The kinetic parameters k_n, k_g, D, i, and j, have been determined for the NQ-DMF-Versamid system in this study, thus permitting prediction of crystallizer performance with various crystallizer designs.

V. CONCLUSIONS

1. High bulk density NQ crystals can be produced from a NQ-DMF-Versamid system in a continuous mixed suspension mixed product removal crystallizer. Bulk densities ranged from 0.92 to 1.05 g/cm^3 for the operating conditions used.

2. The effect of the agitator speed, growth rate, and solids concentration on the nucleation rate was determined using a multiple linear regression technique. The resulting equation is: $B_o = 0.19\ (rpm)^{1.54}\ (G)^{1.68}\ (M_T)^{0.09}$. This result is consistent with postulated secondary nucleation mechanisms.

3. The kinetic parameters $k_n = 0.19$, $k_g = 57.1$, $D = 1.54$, $i = 1.68$, and $j = 0.09$, have been determined for the NQ-DMF-Versamid system. Coupling these parameters with the population and mass balances, crystallizer performance for various crystallizer designs can be predicted.

ACKNOWLEDGEMENTS

I express my appreciation to A. Popolato, J. B. Panowski, and H. L. Flaugh, Group WX-3, for the helpful discussions in the preliminary design and layout of the crystallizer system.

I am very grateful to P. G. Salgado, WX-3, for his assistance and suggestions in performing the experimental work described in this report. His patience and encouragement were very much appreciated during the writing of the manuscript. The timely discussion of the results with A. D. Randolph, visiting Staff Member at Los Alamos Scientific Laboratory, was helpful and tremendously appreciated.

I express my appreciation to C. C. Maxwell, E. Velarde, and L. E. Naranjo, technicians at WX-3, who helped to build and operate the apparatus. Also I wish to thank G. E. Mortenson, WX-3, for his efforts in photographing the crystals.

REFERENCES

1. A. F. McKay, Chem. Rev. 51, 301 (1952).

2. L. Jousselin, Compt. Rend. 88, 814 (1879).

3. T. Ewan and J. H. Young, J. Soc. Chem. Ind. 40, 109T (1921).

4. W. C. McCrone, Anal. Chem. 23, 205 (1951).

5. G. H. Messerly, Office of Scientific Research and Development 1219, 5 (1943).

6. M. J. Urizar, E. James, and L. C. Smith, Physics of Fluids 4, 262 (1961).

7. E. J. Pritchard and G. F. Wright, Can. J. Res. 25, 257 (1947).

8. G. A. Cave, N. J. Krutinger, and J. D. McCaleb, Ind. Eng. Chem 41, 1286 (1949).

9. A. D. Randolph and M. A. Larson, A. I. Ch. E. J. 8, 639 (1962).

10. A. D. Randolph and M. A. Larson, Theory of Particulate Processes (Academic Press, New York and London, 1971).

11. M. A. Larson and A. D. Randolph, Chemical Engineering Progress Symposium Series 65, 1 (1969).

12. A. D. Randolph, Can. J. Chem. Eng. 42, 280 (1964).

13. W. L. McCabe, Ind. Eng. Chem. 21, 112 (1929).

14. M. A. Larson, D. C. Timm, and P. R. Wolff, A. I. Ch. E. J. 14, 448 (1968).

15. Y. A. Liu and G. D. Botsaris, paper presented at American Institute of Chemical Engineers Annual Meeting, Chicago, Illinois, November 1970.

16. S. M. Shor and M. A. Larson, Chemical Engineering Progress Symposium Series 67, 32 (1971).

17. G. R. Youngquist and A. D. Randolph, A. I. Ch. E. J. 18, 421 (1972)

18. R. E. A. Mason and R. F. Strickland-Constable, Trans. Faraday Soc. 62, 455 (1966).

19. N. A. Clontz and W. L. McCabe, Chemical Engineering Symposium Series, 67, 6 (1971).

20. J. N. Robinson and J. E. Roberts, Can. J. Chem. Eng. 35, 105 (1957).

21. H. Lee and K. Neville, Epoxy Resins (McGraw-Hill Book Co., New York, 1957) p. 168.

APPENDIX

CUMULATIVE SIZE DISTRIBUTION PLOTS

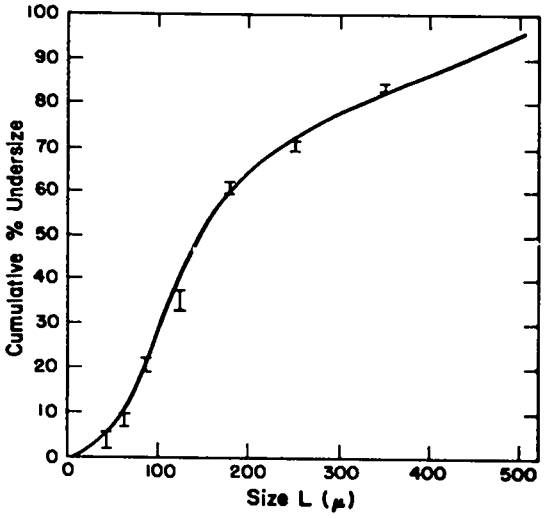

Fig. A-1. Run 7.

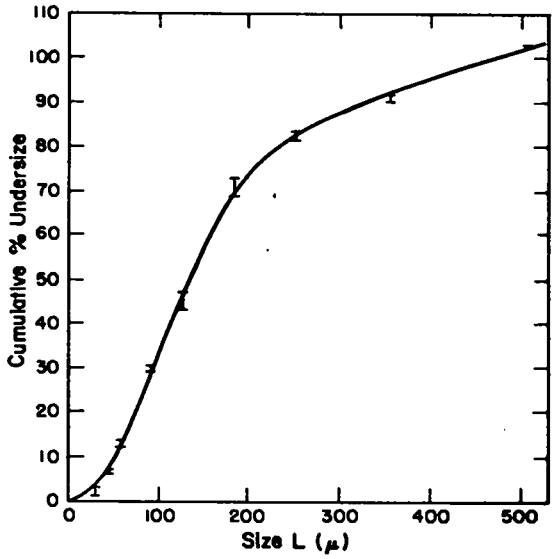

Fig. A-2. Run 8

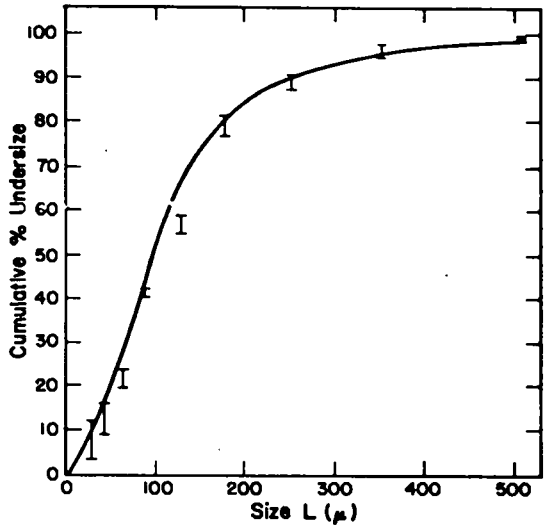

Fig. A-3. Run 9.

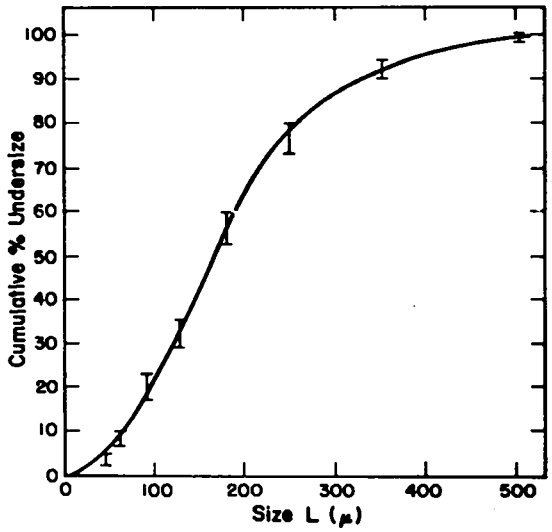

Fig. A-4. Run 10.

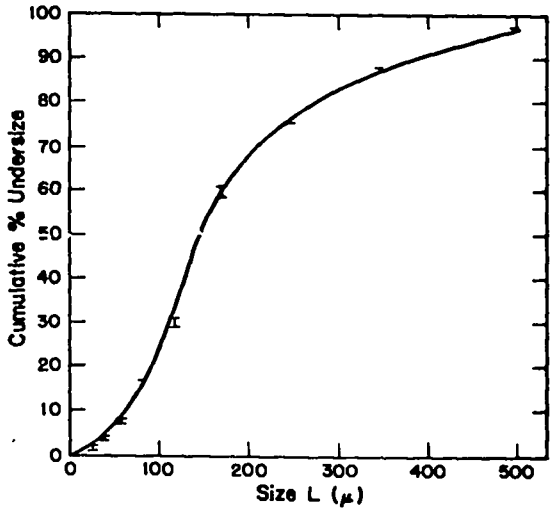

Fig. A-5. Run 11.

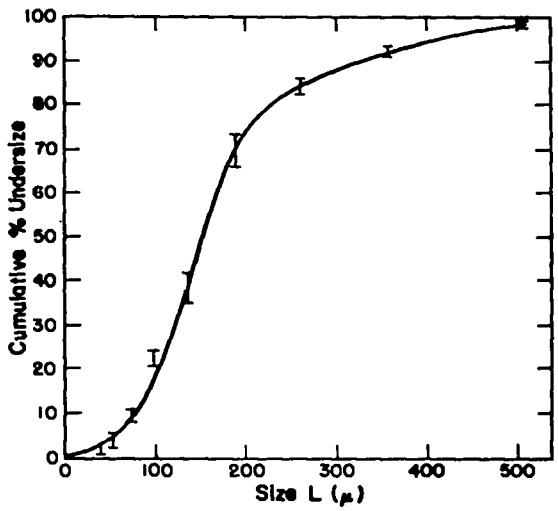

Fig. A-6. Run 12